Published OnlineFirst December 21, 2010; DOI: 10.1158/1535-7163.MCT-10-0574

Preclinical Development

Molecular Cancer Therapeutics

# ENMD-2076 Is an Orally Active Kinase Inhibitor with Antiangiogenic and Antiproliferative Mechanisms of Action

Graham C. Fletcher[1], Richard D. Brokx[1], Trisha A. Denny[1], Todd A. Hembrough[2,3], Stacy M. Plum[2], William E. Fogler[2], Carolyn F. Sidor[2], and Mark R. Bray[1]

## Abstract

ENMD-2076 is a novel orally active, small molecule kinase inhibitor with a mechanism of action involving several pathways key to tumor growth and survival: angiogenesis, proliferation, and the cell cycle. ENMD-2076 has selective activity against the mitotic kinase Aurora A, as well as kinases involved in angiogenesis (VEGFRs, FGFRs). ENMD-2076 inhibited the growth *in vitro* of a wide range of human solid tumor and hematopoietic cancer cell lines with $IC_{50}$ values ranging from 0.025 to 0.7 μmol/L. ENMD-2076 was also shown to induce regression or complete inhibition of tumor growth *in vivo* at well-tolerated doses in tumor xenograft models derived from breast, colon, melanoma, leukemia, and multiple myeloma cell lines. Pharmacodynamic experiments *in vivo* showed that in addition to inhibiting Aurora A, single doses of ENMD-2076 had sustained inhibitory effects on the activation of Flt3 as well as the angiogenic tyrosine kinases, VEGFR2/KDR and FGFR1 and 2. ENMD-2076 was shown to prevent the formation of new blood vessels and regress formed vessels *in vivo* at doses equivalent to those that gave substantial activity in tumor xenograft models. These results indicate that ENMD-2076 is a well-tolerated, orally active multitarget kinase inhibitor with a unique antiangiogenic/antiproliferative profile and provides strong preclinical support for use as a therapeutic for human cancers. Several phase 1 studies involving ENMD-2076 have been recently completed, and the compound is currently being evaluated in a phase 2 clinical trial in patients with platinum-resistant ovarian cancer. *Mol Cancer Ther; 10(1); 126–37. ©2010 AACR.*

## Introduction

At present, a steadily growing number of small molecule and antibody kinase inhibitor drugs have entered the market for use in various colorectal, non–small cell lung, head and neck, renal, breast, and liver cancers, as well as gastrointestinal stromal tumors and chronic myeolcytic leukemia. This class of agents is used both in combination regimens and as single agents (1–3). However, it has become evident that resistance mechanisms such as host mutations quickly render highly specific therapeutic agents ineffective (4). The situation encountered in chronic myeolcytic leukemia where a single kinase drives the pathology of the disease is rare (5), and more commonly, the mechanistic basis for tumorigenesis is multifactorial. The therapeutic utility of a targeted agent used as a single agent can thereby be limited. For example, trastuzumab, an antibody with highly selective affinity for a single kinase, has no activity in a large subset of patients who overexpress the HER2/neu target, for no known reason (6).

This reality has led to several strategies for expanding the utility of kinase inhibitor drugs. One strategy involves rational drug combinations designed to attack several key mechanisms contributing to cancer growth and survival simultaneously such as angiogenesis and proliferation. Another involves the development of compounds that cover multiple mechanisms within a single agent. The first generation of these multitarget kinase drugs (e.g., sunitinib, sorafenib) has validated the multitarget approach and resulted in effective drugs that address significant unmet medical needs. This approach has several potential advantages over combination strategies, including simplicity of the development path, speed to market, and less overlap of side effects. A balance must be maintained, however, between activity toward the desired targets and maintaining an acceptable safety profile.

In this study, we have characterized the properties of ENMD-2076, a novel small molecule multitarget kinase inhibitor. We show here that ENMD-2076 inhibits a unique profile of tyrosine kinase targets, in addition to Aurora A which is a key regulator of the process of

**Authors' Affiliations:** [1]Preclinical Sciences, EntreMed, Inc., Toronto, Ontario, Canada; [2]Cell Biology, EntreMed, Inc.; and [3]Expression Pathology Inc., Rockville, Maryland

**Note:** Supplementary material for this article is available at Molecular Cancer Therapeutics Online (http://mct.aacrjournals.org/).

**Corresponding Author:** Mark R. Bray, Entremed Inc., 101 College Street, Toronto, Ontario, Canada M5G 1L7. Phone: 416-581-7570; Fax: 416-204-2276. E-mail: markb@entremed.com

**doi:** 10.1158/1535-7163.MCT-10-0574

Published OnlineFirst December 21, 2010; DOI: 10.1158/1535-7163.MCT-10-0574



mitosis and is often overexpressed in human cancers (7, 8). ENMD-2076 is shown to have substantial impact on several of the most important pathways involved in mitosis and angiogenesis and inhibition of these processes is likely to contribute to the substantial antitumor activity of the compound as a single agent at well-tolerated doses in a variety of preclinical tumor models.

## Materials and Methods

### Reagents

ENMD-2076 free base was synthesized as described (9) and converted to a tartrate salt. Antibodies used were Thr288 phosphorylated Aurora A, Ser10 phosphorylated Histone H3, Kit, phosphorylated Thr288 Aurora A/Thr232 Aurora B/Thr198 Aurora C, Tyr1175 phosphorylated VEGFR2/KDR (Cell Signaling Technology); Flt3, TACC3 (Santa Cruz Biotechnology); Tubulin, 4G10 phosphorylated tyrosine residues (Millipore); MPM2 (Abcam), NuMA (EMD Biosciences), CD31 (BD Biosciences); goat anti-mouse IgG IRDye 680 and goat anti-rabbit IgG IRDye 800 secondary antibodies (LI-COR Biosciences); sheep anti-mouse IgG and donkey anti-rabbit HRP-labeled secondary antibodies (GE Healthcare).

### Kinase assays

Recombinant Aurora A and B kinase enzymes and appropriate PanVera Z'-Lyte kinase assay kits were purchased from Invitrogen. Assays were carried out in kinase assay buffer (50 mmol/L of HEPES, pH 7.5, 10 mmol/L of $MgCl_2$, 5 mmol/L of EGTA, 0.05% Brij-35) supplemented with 2 mmol/L of DTT, according to the manufacturer's instructions. Activities were determined at an ATP concentration equivalent to the apparent $K_m$ for each enzyme, and an enzyme concentration that resulted in approximately 30% phosphorylation of the peptide substrate after 1 hour. Dose–response curves of relative enzyme activity versus ENMD-2076 concentration were plotted with Grafit (Erithacus Software) and used to calculate $IC_{50}$ values. Potency of ENMD-2076 free base against a select panel of 100 kinase enzymes was determined using the SelectScreen kinase profiling service (Invitrogen). ATP concentrations were at the apparent $K_m$ for each enzyme, or 100 μmol/L if the apparent $K_m$ could not be reached. Percent inhibition was determined at an ENMD-2076 free base concentration of 1 μmol/L; for kinases where significant inhibition was noted, $IC_{50}$ values were determined by generating full 10-point dose–response curves.

### Cell and proliferative assays

All cell lines were obtained from and cultured as recommended by American Type Culture Collection and were classified by short-tandem repeat profiling. Cell lines were routinely tested for mycoplasma and used at low passage numbers (<10). The antiproliferative effect of ENMD-2076 on adherent tumor cell lines was measured by plating 500 cells per well in a 96-well plate and incubating with 9 doses of compound, spanning 0.3 nmol/L to 125 μmol/L, for 96 hours. Cellular proliferation was measured using the sulforhodamine B (SRB; Sigma Aldrich) assay (10). The leukemia-derived, nonadherent cell lines were assayed by plating 5,000 cells per well in a 96-well plate. The cells were incubated with 9 doses of compound, spanning 0.3 nmol/L to 125 μmol/L, for 48 hours and then survival was assayed using the Alamar Blue reagent (Invitrogen) according to the manufacturer's instructions. To measure the effect of ENMD-2076 on VEGF- and fibroblast growth factor (FGF)-induced proliferation of human umbilical vein endothelial cell (HUVEC), cells were serum starved for 6 hours, then treated with ENMD-2076 free base, and stimulated with 5 ng/mL bFGF or 25 ng/mL VEGF (R and D Systems) for 72 hours. Cell proliferation was measured using WST-1 (Roche Applied Science) according to the manufacturer's instructions.

### Immunoblotting and immunoprecipitation

Protein phosphorylation was examined either by fractionation of whole-cell lysates (Aurora A, B, and C, Histone H3, VEGFR2/KDR, and FRS2) or by immunoprecipitation prior to fractionation (Flt3, Kit, CSF1R). To arrest cells at $G_2$-M phase to enrich for Aurora A, Aurora B, and phosphorylated histone H3 content, cells were incubated with 0.5 μg/mL nocodazole (Sigma Aldrich) for 16 hours. For whole-cell lysates, cells were treated as indicated in the text, washed in cold PBS, and then lyzed in ice-cold 50 mmol/L of Tris-HCl, pH 7.5, 1% Triton X-100, 10% glycerol, 100 mmol/L of NaCl, 2.5 mmol/L of EDTA supplemented with 10 μg/mL leupeptin and aprotinin, 2 μg pepstatin, 2 mmol/L of PMSF, 1 mmol/L of NaF, 0.5 mmol/L of sodium orthovanadate, and 8 mmol/L of β-glycerol phosphate. Adherent cells were scraped off the plate, transferred to an eppendorf, sonicated, and the lysates cleared by centrifugation at 20,000 × *g* at 4°C. The protein concentration was determined by bicinchoninic acid protein assay (Pierce) and 40 μg of protein per sample was resolved using 4% to 12% NuPage Bis-Tris gels (Invitrogen), transferred to nitrocellulose membrane, and then probed with antibodies as indicated in the text. For immunoprecipitation experiments, cells were treated as indicated in the text, washed in cold PBS, and then lyzed in 20 mmol/L of Tris-HCl, 150 mmol/L of NaCl, 1 mmol/L of EGTA, 1 mmol/L of EDTA, 1% Triton X-100, 2.5 mmol/L of sodium pyrophosphate supplemented with 10 μg/mL leupeptin and aprotinin, 2 μg pepstatin, 2 mmol/L of PMSF, 1 mmol/L of NaF, 0.5 mmol/L of sodium orthovanadate, and 8 mmol/L β-glycerol phosphate. Adherent cells were scraped off the plate, transferred to a microcentrifuge tube, sonicated on ice, and centrifuged at 20,000 × *g* at 4°C. The protein concentration was determined by bicinchoninic acid protein assay and the volume of supernatant containing a total of 400 μg protein was incubated with

Published OnlineFirst December 21, 2010; DOI: 10.1158/1535-7163.MCT-10-0574



primary antibody for 16 hours and then protein A agarose beads (Invitrogen) were added for 1 hour. The sample was then washed 4 times by repeated cycles of microcentrifugation for 30 seconds at 4°C and resuspension in 500 μL of 1× cell lysis buffer. After the final wash, 20 μL of 1.5× SDS sample buffer was added to the pelleted beads and the sample was vortexed, heated to 95°C to 100°C for 5 minutes, microcentrifuged for 1 minute at 20,000 × *g* and analyzed by Western blotting as outlined above. To determine phosphorylation levels of Histone H3 and Aurora A, B, and C, the membranes were incubated with an infrared fluorescent secondary antibody (LI-COR Biosciences) and then $IC_{50}$ values were calculated from quantification of the bands using the Odyssey Infrared Imaging System and analytical software (LI-COR Biosciences). To determine phosphorylation levels of Flt3, Kit, VEFGR2/KDR, FRS2, and CSF1R, the membranes were incubated in a horseradish peroxidase-labeled secondary antibody (GE Healthcare) and developed by enhanced chemiluminescence. Band intensity was quantified by densitometry (ChemiDoc XRS, Bio-Rad) and used to calculate $IC_{50}$ values.

### Animals

All animals were supplied by Taconic Labs and housed in a barrier facility. In conducting the research in this report, the investigators adhered to the principles of Laboratory Animal Care (NIH Publication No. 85-23).

### Vascular invasion into matrigel plug *in vivo*

C57B16 mice were injected with 500 μL of Matrigel (BD Biosciences) premixed with 0 or 0.5 μg/mL of bFGF and orally treated with ENMD-2076 free base as indicated. At the end of the study, mice were infused intravenously with 200 μL of FITC (fluorescein isothiocyanate)-Dextran (10 mg/mL; Sigma Aldrich) and 20 minutes later, Matrigel plugs were surgically removed and placed in 10% neutral-buffered formalin (Sigma Aldrich) for 16 hours, then washed in PBS, homogenized, and quantified in a 96-well fluorescent plate reader. Representative sections were imaged using an Olympus 1 × 70 microscope to show the amount of vascular invasion.

### Xenograft models

Cell lines (generally, $1 \times 10^6$ to $5 \times 10^6$ cells) were injected subcutaneously or into the mammary fat pad (MDA-MB-231 only) of 5- to 6-week-old CB.17 SCID or NCr nude mice. Tumors were allowed to grow for 10 to 50 days before drug treatment was initiated at the tumor volumes indicated in Table 1. All treatments were with ENMD-2076 in water or ENMD-2076 free base in CMC-Tween vehicle (0.075% carboxymethylcellulose, 0.085% Tween 80 in water), administered orally. Multiple experiments indicated that the 2 are virtually identical on a molar basis (data not shown); to calculate an equivalent dose of ENMD-2076, multiply the amount of ENMD-2076 free base used by 1.51. Percent tumor growth inhibition was calculated by the formula:

$$\%\,\mathrm{TGI} = 100 \times [1 - (\mathrm{TV}_{\mathrm{f,\,treated}} - \mathrm{TV}_{\mathrm{i,\,treated}}) / (\mathrm{TV}_{\mathrm{f,\,control}} - \mathrm{TV}_{\mathrm{i,\,control}})]$$

In cases where regression occurred, percent regression was calculated by the formula:

$$\%\,\mathrm{Regression} = 100 \times [1 - (\mathrm{TV}_{\mathrm{f,\,treated}} / \mathrm{TV}_{\mathrm{i,\,treated}})]$$

where $TV_f$ is the average tumor volume at end of study and $TV_i$ is the average tumor volume at the initiation of treatment.

### *In vivo* pharmacodynamic studies

The effect of ENMD-2076 treatment on the activity of target kinases was determined in subcutaneous xenografts of cancer cell lines expressing the desired target. Briefly, $2 \times 10^6$ to $30 \times 10^6$ cells mixed with Matrigel were injected subcutaneously into NCr nude or CB.17 SCID mice, tumors were grown to an appropriate size (approximately 500–750 $mm^3$) and were then treated with a single dose of ENMD-2076 administered orally in water. After the time indicated, tumors were snap frozen on dry ice and homogenized with a tissue grinder in freshly prepared cell lysis buffer (25 mmol/L of HEPES, 1.5 mmol/L of $MgCl_2$, 0.2 mmol/L of EDTA, 0.1% Triton X-100, 0.3 mmol/L of NaCl, 1 mmol/L of DTT, 1 mmol/L of $Na_3V0_4$, 20 mmol/L of NaF, 0.01 mg/mL aprotinin; 12.5 μmol/L of leupeptin; 1 mmol/L of PMSF, 20 mmol/L of β-glycerophosphate) supplemented with a Complete Mini protease inhibitor tablet (Roche Applied Science). Inhibition of target kinase phosphorylation was analyzed by immunoprecipitation (Flt3, VEGFR2/KDR, FGFR1, FGFR2), or Western blotting (STAT5) of tumor lysates as outlined above, and samples from 3 or 4 individual animals were run. Immunofluorescence was used to follow Aurora A activity. For this experiment, HT29 tumors were extracted 8 hours after treatment, fixed in 4% parformaldehyde for 16 hours, and then paraffin embedded and sectioned. Tissue sections were probed with either mouse primary antibody (NuMA or MPM2) or rabbit primary antibody (phosphorylated Aurora A or TACC3) overnight, then washed 3 times in PBS. Sections were then incubated in fluorescently labeled goat anti-rabbit-Alexa488 or goat anti-mouse rhodamine secondary antibodies (Invitrogen) for 1 hour and then washed 3 times in PBS before mounting and imaging using an Olympus 1×70 microscope. To stain for vasculature using the CD31 marker, resected tumors were fixed for 16 hours in neutral-buffered formalin, then paraffin embedded and sectioned. Sections were incubated in xylenes to remove paraffin and then rehydrated through incubation in graded ethanol solutions. Antigen retrieval was done by incubation in 20 μg/mL proteinase K (Roche Applied Sciences) for 20 minutes at room temperature. Endogenous peroxidases were quenched by incubation in 3% hydrogen peroxide (Sigma Aldrich) in methanol for 20 minutes and then sections were probed overnight with rat anti-CD31 antibody. CD31 was visualized using

Published OnlineFirst December 21, 2010; DOI: 10.1158/1535-7163.MCT-10-0574



**Table 1.** Antitumor efficacy of ENMD-2076 in xenograft models

| Model | Initial tumor volume, $mm^3$ (d) | Dose, mg/kg | % TGI (day of treatment) | Regressions | % Regression (day of treatment) | Comments |
|---|---|---|---|---|---|---|
| HCT-116 colon carcinoma | 200 (10) | 100[a] b.i.d. | 89 (20) | 0/9 | | |
| | | 200[a] b.i.d. | | 7/7 | 54 (20) | 2/9 deaths |
| HT29 colon carcinoma | 400 (18) | 50 q.d. | 57 (27) | 0/8 | | |
| | | 100 q.d. | 62 (27) | 4/8 | | |
| | | 200 q.d. | 90 (27) | 7/8 | | |
| CT-26 syngeneic mouse colon carcinoma | 120 (9) | 50 q.d. | −8 (26), NS | 0/10 | | |
| | | 100 q.d. | 21 (26), NS | 0/8 | | |
| | | 200 q.d. | 24 (26), NS | 0/7 | | |
| A375 melanoma | 100 (21) | 35 q.d. | 13 (18), NS | 0/10 | | |
| | | 76 q.d. | 42 (18), NS | 0/10 | | |
| | | 151 q.d. | 81 (18) | 0/10 | | |
| | | 302 q.d. | 98 (18) | 3/9 | | 1/10 death; drug was held from d 13–16 |
| MDA-MB-231 mammary orthotopic | 150 (21) | 50[a] q.d. | 62 (27) | 0/8 | | |
| | | 100[a] q.d. | 94 (27) | 1/8 | | |
| | | 200[a] q.d. | 99 (27) | 4/8 | | |
| | 300 (32) | 75 q.d. | 54 (18) | 0/10 | | |
| | | 302 q.d. | 99 (18) | 4/10 | | |
| | 450 (33) | 200 q.d. | 96 (17) | 1/9 | | |
| | 1740 (50) | 200 q.d. | | 7/9 | 54 (14) | |
| H929 multiple myeloma | 300 (18) | 75 q.d. | 69 (20) | 0/5 | | |
| | | 150 q.d. | 88 (20) | 0/4 | | |
| | | 225 q.d. | 88 (20) | 0/5 | | |
| OPM-2 multiple myeloma | 200 (20) | 75 q.d. | 56 (10) | 0/6 | | |
| | | 150 q.d. | 59 (10) | 1/6 | | |
| | | 225 q.d. | 86 (10) | 1/6 | | |
| | 900 (30) | 225 q.d. | | 4/4 | 65 (11) | |
| MV4;11 acute myelogenous leukemia | 450 (34) | 50[a] q.d. | | 4/6 (3/6 PR, 1/6 CR) | 32 (25) | |
| | | 100[a] q.d. | | 6/6 (4/6 PR, 2/6 CR) | 96 (25) | |
| | | 150[a] q.d. | | 6/6 (4/6 PR, 2/6 CR) | 99 (25) | |
| | | 25[a] b.i.d. | 99 (25) | 3/6 (3 PR) | | |
| | | 50[a] b.i.d. | | 5/6 (4/6 PR, 1/6 CR) | 83 (25) | |
| HL60 acute promyelocytic leukemia | 700 (36) | 75[a] q.d. | 77 (27) | 2/8 | | |
| | | 150[a] q.d. | 83 (27) | 3/7 | | |

NOTE: Treatment was initiated after the stated number of days when the specified tumor volume was reached. Animals were dosed with ENMD-2076 in water unless otherwise indicated.

Abbreviations: TGI, tumor growth inhibition; b.i.d., twice a day dosing; q.d., once a day dosing; NS, not significant; PR, partial regression; and CR, complete regression.

[a]In these studies, the compound used was the free base of ENMD-2076 formulated in 0.075% carboxymethylcellulose, 0.085% Tween 80 in water. Data on file indicate that the 2 compounds have equivalent biological activity on a molar basis. To calculate an equivalent dose of ENMD-2076, multiply by 1.51.

Published OnlineFirst December 21, 2010; DOI: 10.1158/1535-7163.MCT-10-0574



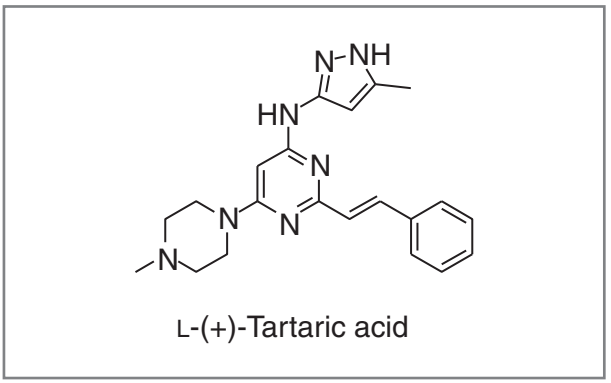


Figure 1. ENMD-2076 structure and properties. Chemical structure of ENMD-2076.

horseradish peroxidase catalysis of diaminobenzidine using the Tyramide amplification system (Perkin Elmer) according to the manufacturer's instructions.

## Results

### Discovery and *in vitro* characterization of ENMD-2076

ENMD-2076 is the tartrate salt of a vinyl-pyrimidine free base previously referred to as ENMD-981693 or MKC-1693 (Fig. 1). In assays against recombinant human kinases, ENMD-2076 inhibits Aurora A with an $IC_{50}$ value of 14 nmol/L and is selective toward Aurora A versus Aurora B ($IC_{50} = 350$ nmol/L; Table 2). The activity of ENMD-2076 on other kinases, including clinically relevant mutant kinases, was assessed by screening against a panel of 100 kinases at a concentration of 1 μmol/L (Supplementary Table S1A). Less than 50% inhibition at 1 μmol/L was seen for most of these kinases. $IC_{50}$ values were determined by 10-point titration curve analysis for 30 kinases where there was greater than 75% inhibition in the initial screen (Supplementary Table S1B). Fifteen kinases displayed $IC_{50}$ values of less than 100 nmol/L. Among these were multiple kinases involved in angiogenesis, including VEGFR2/KDR and VEGFR3, FGFR1 and FGFR2, and PDGFRα (Table 3).

The activity of ENMD-2076 was evaluated against cell lines derived from both hematologic and solid tumors in *in vitro* assays (Tables 4 and 5). Using a panel of 7 solid tumor cell lines in a 4-day assay, $IC_{50}$ values between 0.12 and 0.7 μmol/L with a mean $IC_{50}$ value of 0.4 μmol/L were obtained. ENMD-2076 inhibited HUVEC growth with an $IC_{50}$ value of 0.15 μmol/L. Against 10 human leukemia cell lines, the $IC_{50}$ values ranged from 0.025 to 0.53 μmol/L (Table 5). Within this panel, MV4;11 cells were the most sensitive cells by a factor of greater than 4. Flow cytometric analysis of the lymphoma-derived U937 cell line treated with ENMD-2076 showed that the compound induced a dose-dependent increase in $G_2$-M-phase arrest as well as the induction of apoptosis (Supplementary Fig. S1), which is consistent with the

**Table 2.** ENMD-2076 is selective against Aurora A compared with Aurora B, $IC_{50}$ of ENMD-2076 against Aurora A and Aurora B

| Kinase | $IC_{50}$ (nmol/L) |
|---|---|
| Aur A | 14 ± 4.6 ($n = 83$) |
| Aur B | 350 ± 160 ($n = 19$) |

**Table 3.** ENMD-2076 is active against multiple oncogenic kinases.

| Kinase | $IC_{50}$ (nmol/L) |
|---|---|
| FLT3 | 1.86 |
| RET | 10.4 |
| FLT4 (VEGFR3) | 15.9 |
| SRC | 20.2 |
| NTRK1 (TRKA) | 24.2 |
| CSF1R (FMS) | 24.8 |
| LCK | 43.7 |
| PTK2 (FAK) | 54.9 |
| PDGFRα | 56.4 |
| KDR (VEGFR2) | 58.2 |
| BLK | 69.4 |
| FGFR2 | 70.8 |
| YES1 | 78.4 |
| ABL1 T315I | 81.3 |
| FGFR1 | 92.7 |
| FYN | 112 |
| JAK2 | 120 |
| KIT | 120 |

Note: $IC_{50}$ of ENMD-2076 against multiple oncogenic kinases; the 18 most potent kinases from the 30 kinases screened are shown.

**Table 4.** Antiproliferative activity of ENMD-2076 versus solid tumor cell lines and HUVECs.

| Cell line | $IC_{50}$ (μmol/L) |
|---|---|
| PANC-1 | 0.12 |
| HCT116 | 0.2 |
| A549 | 0.26 |
| HT-29 | 0.4 |
| MCF7 | 0.55 |
| PC-3 | 0.6 |
| BXPC-3 | 0.7 |
| HUVEC | 0.15 |

Published OnlineFirst December 21, 2010; DOI: 10.1158/1535-7163.MCT-10-0574



**Table 5.** Antiproliferative activity of ENMD-2076 versus human leukemia cell lines

| Cell line | $IC_{50}$ (μmol/L) |
|---|---|
| MV4:11 | 0.025 |
| U937 | 0.12 |
| Kasumi | 0.135 |
| MO7e | 0.185 |
| HL-60 | 0.27 |
| TF-1 | 0.36 |
| Jurkat | 0.44 |
| K562 | 0.45 |
| THP-1 | 0.45 |
| Hel 92.1.7 | 0.53 |

selective inhibition of Aurora A rather than Aurora B, as the inhibition of Aurora B would have resulted in endoreduplication and an accumulation of cells greater than 4N (11, 12).

### Inhibition of cellular kinases by ENMD-2076

Phosphospecific antibodies and cell lines endogenously expressing the kinase of interest were employed to examine the inhibition of putative targets of ENMD-2076 in a cellular context. The cellular activity of Aurora kinase A and B was followed in HCT116 cells that had been arrested at $G_2$-M phase by incubation with nocodazole (Fig. 2A). A cellular $IC_{50}$ value of 0.13 μmol/L was obtained for Aurora A and a cellular $IC_{50}$ value of 0.45 μmol/L was obtained for Aurora B. The value for Aurora C, which is closely related to Aurora B (13), was 0.53 μmol/L, and the value for the Aurora B substrate Histone H3 (14) was 0.65 μmol/L. Thus, consistent with the *in vitro* kinase assay results, ENMD-2076 has selectivity for Aurora A over Aurora B in cells *in vitro*. Aurora A is involved in centrosomal maturation and separation and mitotic spindle formation. Intercentrosomal distance was measured to determine whether Aurora A function is inhibited in cells (15, 16). When cells were treated with ENMD-2076 *in vitro*, the average intercentrosomal distance decreased from 12.0 μm without ENMD-2076 to 5.1 and 3.1 μm with 0.2 and 2 μmol/L of ENMD-2076, respectively (Supplementary Fig. S2). Abnormal mitotic spindle formation was also seen with ENMD-2076 treatment. Together, these results are consistent with ENMD-2076 selectively inhibiting Aurora A activity in cells.

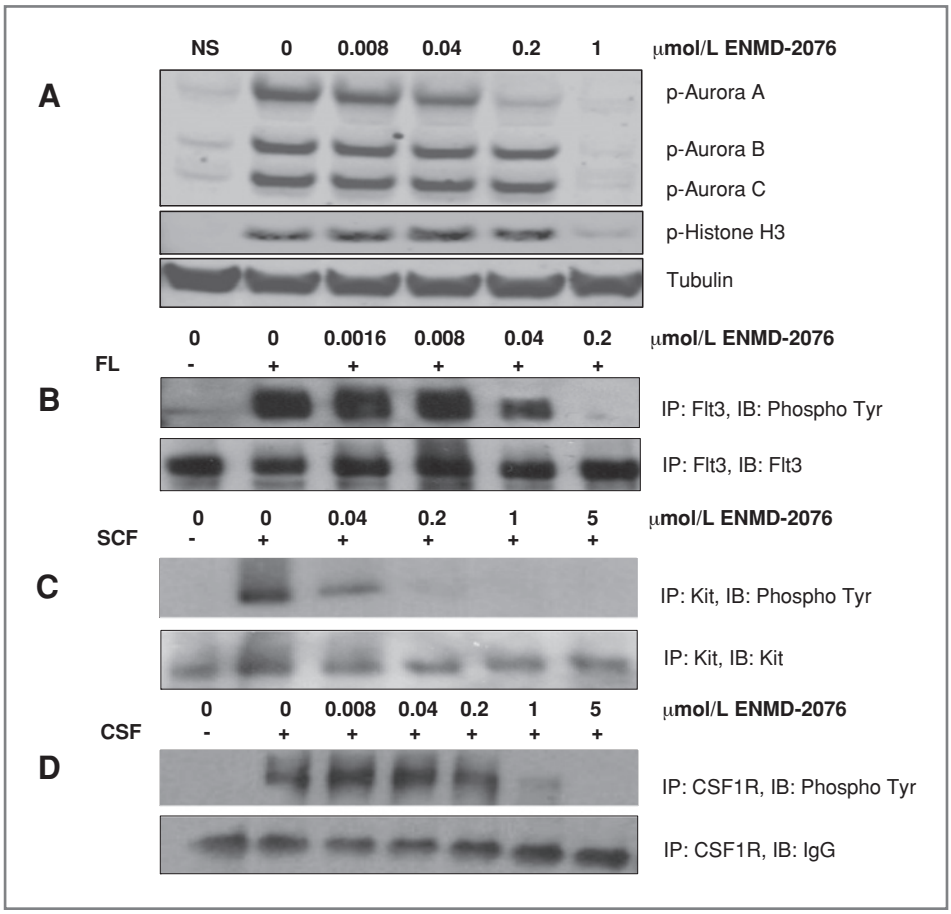


**Figure 2.** ENMD-2076 inhibits cellular Aurora A, Flt3, Kit, and CSF1R. A, HCT116 cells arrested at $G_2$/M phase were incubated for 2 hours with ENMD-2076 and Aurora activity was examined by Western blotting of whole-cell lysates followed by probing with an antibody specific for the active, phosphorylated Thr288, Thr232, and Thr198 residue on Aurora A, B, and C, respectively, and for phosphorylated Ser10, on histone H3 and tubulin. B, inhibition of FL-stimulated Flt3 phosphorylation in THP-1 cells. C, inhibition of SCF-stimulated Kit phosphorylation in MO7e cells. D, inhibition of CSF-stimulated CSF1R phosphorylation in MV4;11 cells. For B–D, cells were incubated with ENMD-2076 free base for 1 hour, stimulated with growth factors for 5 minutes, proteins were immunoprecipitated, and then protein phosphorylation was analyzed by probing with the 4G10 anti-phosphotyrosine antibody. Sample loading is shown by stripping and reprobing with anti-Flt3 (B) or anti-Kit (C) or through a nonspecific IgG band (D).

Published OnlineFirst December 21, 2010; DOI: 10.1158/1535-7163.MCT-10-0574



In addition to the *in vitro* activity of ENMD-2076 against Aurora A and B, the compound also inhibited kinases that could be involved in oncogenesis, including Flt3, Kit, and CSF1R. To understand better the potential contribution of the inhibition of these kinases to the mechanism of action of ENMD-2076, the potency of ENMD-2076 against these targets within a cellular context was determined (Fig. 2). Flt3 and Kit are both members of the PDGFR-family. Flt3 is constitutively activated, either through a point mutation or internal tandem duplications of the juxtamembrane domain, in about one third of all acute myeloid leukemia (AML) patients (17). ENMD-2076 inhibited cellular Flt3 ligand (FL)-induced Flt3 autophosphorylation in THP-1 cells, which have been shown to express FL-responsive wild-type Flt-3 (18) with an $IC_{50}$ value of 28 nmol/L (Fig. 2B). Kit plays a critical role in cell growth, differentiation, development, and survival in multiple cell types including hematopoietic stem cells, melanocytes and germ cells, and constitutively activating mutations of *c-KIT* can cause mastocytosis, gastrointestinal stromal tumors, AML, and testicular tumors (19). To examine the inhibition of Kit by ENMD-2076 MO7e cells, which express wild-type Kit and are dependent on Kit signaling for proliferation and survival (20) were used. ENMD-2076 inhibited stem cell factor (SCF)-induced Kit autophosphorylation in MO7e cells with an $IC_{50}$ value of 40 nmol/L (Fig. 2C). CSF1R, also known as the *c-fms* protooncogene, is a receptor tyrosine kinase upregulated in many cancers, including breast, ovarian, prostate, and endometrial (21), and the inhibition of CSF1R signaling decreases mammary tumor growth in mice (22). MV4;11 cells express the CSF1R protein (23) and ENMD-2076 inhibited colony-stimulating factor (CSF)-stimulated CSF1R signaling in these cells with an $IC_{50}$ value of 600 nmol/L (Fig. 2D). In specific instances, activity in the *in vitro* kinase screen was not correlated with activity against the endogenous kinase. For example, ENMD-2076 inhibited Abl and the clinically relevant T315I Abl mutant *in vitro* with $IC_{50}$ values of 295 and 81 nmol/L, respectively; however, ENMD-2076 only partially inhibited Abl and T315I mutant Abl activity within live cells at concentrations of 25 μmol/L and higher (data not shown).

### Inhibition of angiogenic kinases by ENMD-2076

Multiple receptor tyrosine kinases involved in angiogenesis were inhibited by ENMD-2076 in *in vitro* assays (Fig. 1C). The potency of ENMD-2076 on cellular VEGFR2/KDR and FGFRs was assessed using HUVECs (Fig. 3A). ENMD-2076 inhibited VEGFR2/KDR autophosphorylation with an $IC_{50}$ value of 7 nmol/L. FGFR activity was assayed using the phosphorylation status of the FGFR substrate 2 (FRS2) as a reporter and ENMD-2076 inhibited FGFR activity with an $IC_{50}$ value of 600 nmol/L. The inhibition of VEGFR2/KDR and FGFR activity by ENMD-2076 was also assayed by examining inhibition of VEGF- and FGF-stimulated HUVEC cell proliferation. VEGF-induced cell proliferation was inhibited with an $IC_{50}$ value of 76 nmol/L and FGF-induced cell proliferation was inhibited with an $IC_{50}$ value of 139 nmol/L (Fig. 3B). Inhibition of FGFR signaling was also examined *in vivo* in a Matrigel plug assay, where blood vessel growth into the Matrigel plug was stimulated by FGF premixed in the Matrigel prior to implantation in the mice. In this assay, ENMD-2076 dose levels that were efficacious *in vivo* in tumor xenograft models inhibited angiogenic growth into the Matrigel with no discernible toxic effects, when administered at time of implantation onward (Fig. 3C and Supplementary Fig. S3). In addition, in a similar experiment in which compound was administered 1 week following implantation, regression of established vessels was observed (Fig. 3D).

### Antitumor activity of ENMD-2076 *in vivo*

The *in vivo* activity of ENMD-2076 was assessed in multiple cancer cell line xenografts, including models from breast, colon, melanoma, multiple myeloma, and AML, and the results are shown in Table 1. More detailed tumor growth curves and body weight charts are shown in Supplementary Figure S4. In most models, ENMD-2076 treatment resulted in statistically significant, dose-dependent inhibition of tumor growth or tumor regression. Moreover, there was no correlation between tumor growth rate and antitumor efficacy, which would conceivably be expected for a mitotic kinase inhibitor, as fast-growing (e.g., A375 melanoma) and slow-growing (e.g., HT29 colon carcinoma) tumors were similarly inhibited by the compound. These results are consistent with those of other inhibitors of Aurora kinases, such as tozasertib (VX-680/MK0457; ref. 24) and MLN-8054 (25), which also elicited similar responses in various xenograft models with differing growth rates.

The compound was well tolerated at daily doses up to 302 mg/kg (equivalent to 200 mg/kg of the free base), with no weight loss or signs of morbidity noted in any study at this dose with the exception of the A375 model (Table 1). Twice daily dosing schedules up to 200 mg/kg orally were also examined, and although not acutely toxic, morbidity, including weight loss and death of animals, was observed after 7 to 10 days of continuous treatment at this dose level.

### Pharmacodynamic effects of ENMD-2076

To understand which kinase targets of ENMD-2076 may be important for the mechanism of action of ENMD-2076 *in vivo*, multiple subcutaneous models using cell lines expressing the kinase of interest were used (Fig. 4). In all of these experiments, tumor-bearing animals were treated with a single oral dose of ENMD-2076 and representative results of multiple experiments are reported. MV4;11 cells express the Flt-3 internal tandem duplication mutation and are dependent on Flt3 activity for survival (26). A dose of 45 mg/kg inhibited Flt3 activity in MV4;11 tumors on the basis of the phosphorylation status of both Flt3 and the Flt3 substrate STAT5 (27). Inhibition of both phosphorylation events was most

Published OnlineFirst December 21, 2010; DOI: 10.1158/1535-7163.MCT-10-0574



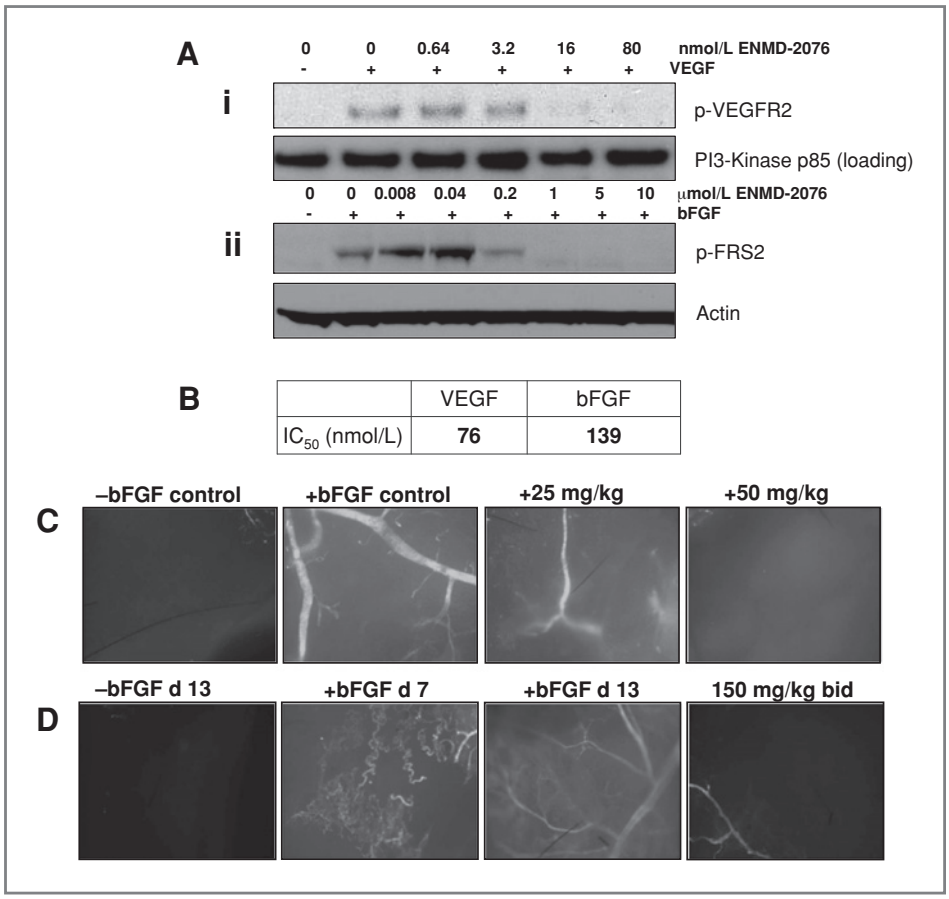


**Figure 3.** Antiangiogenic action of ENMD-2076. A, HUVECs were incubated with ENMD-2076 free base for 1 hour, stimulated with VEGF (i) or bFGF (ii) for 5 minutes, then whole-cell lysates were analyzed by Western blotting. VEGFR2/KDR activity was examined using an antibody specific for the autophosphorylated Tyr1175 site (i). FGFR activity was reported using the phosphorylation status of FRS2 (ii). B, HUVECs were serum starved for 6 hours then treated with ENMD-2076 and stimulated with 5 ng/mL bFGF or 25 ng/mL VEGF for 72 hours. C and D, ENMD-2076 inhibited blood vessel growth and regressed newly established blood vessels in the FGF-driven Matrigel angiogenesis model *in vivo*. C, bFGF-containing Matrigel was injected into mice that were then orally dosed daily with ENMD-2076 free base for 10 days before vessel growth was imaged. D, bFGF-containing Matrigel was injected into animals that were grown for 7 days prior to imaging vessel growth in 1 group of animals. Two other groups of animals were then treated either with or without ENMD-2076 free base for a further 7 days and then vessels were imaged. All panels ×40 magnification, 0.5 seconds exposure.

pronounced at 4 hours but still present 24 hours after dosing (Fig. 4A). VEGFR2/KDR and FGFR1 activity was followed in a MiaPaCa-2 pancreatic cancer model by examining the phosphorylation status of the kinases. Similar inhibition was seen for both kinases, with greater than 60% inhibition 4 hours following a dose of 75 mg/kg and increased inhibition at this time point following a dose of 150 and 225 mg/kg. The level of phosphorylation of both kinases began to return to control levels at 24 and 48 hours, though there is still inhibition 48 hours after treatment (Fig. 4B and C). FGFR2 activity was determined using a xenograft model of KATOIII gastric carcinoma cells which contain an amplified *FGFR2* gene (found in 3%–10% of primary gastric cancers) that results in a dependence on FGFR2 for growth and survival (28). Whereas significant inhibition is visible at 4 hours after treatment only at the 200 mg/kg of dose level, strong inhibition is observed at 24 and 48 hours after treatment with 50, 100, or 200 mg/kg (Fig. 4D).

To determine whether ENMD-2076 inhibited Aurora kinase activity *in vivo*, 2 assays were employed. In the HT29 colorectal model, Aurora A inhibition was followed through specific staining for the phosphorylation at Thr288, an autophosphorylation site reflective of active enzyme (25). Given that Aurora kinases are only present in activated cells undergoing mitosis, several consecutive daily doses were employed to capture a greater number of division cycles within the tumor. Five doses of 200 mg/kg of ENMD-2076 inhibited Aurora A phosphorylation in the cells that were positive for the mitotic marker, mitotic protein monoclonal 2 (MPM2; Fig. 4E). Thirty mitotic nuclei per condition (from 3 different animals) were counted, and ENMD-2076 treatment increased the proportion of MPM2 positive nuclei containing weak or absent phosphorylated Aurora A from 32% to 80%. The second assay to examine Aurora A inhibition *in vivo* was based on the Aurora A-dependent localization of transferring acidic coiled-coil containing protein 3 (TACC3) to the mitotic spindle in mitotically

Published OnlineFirst December 21, 2010; DOI: 10.1158/1535-7163.MCT-10-0574



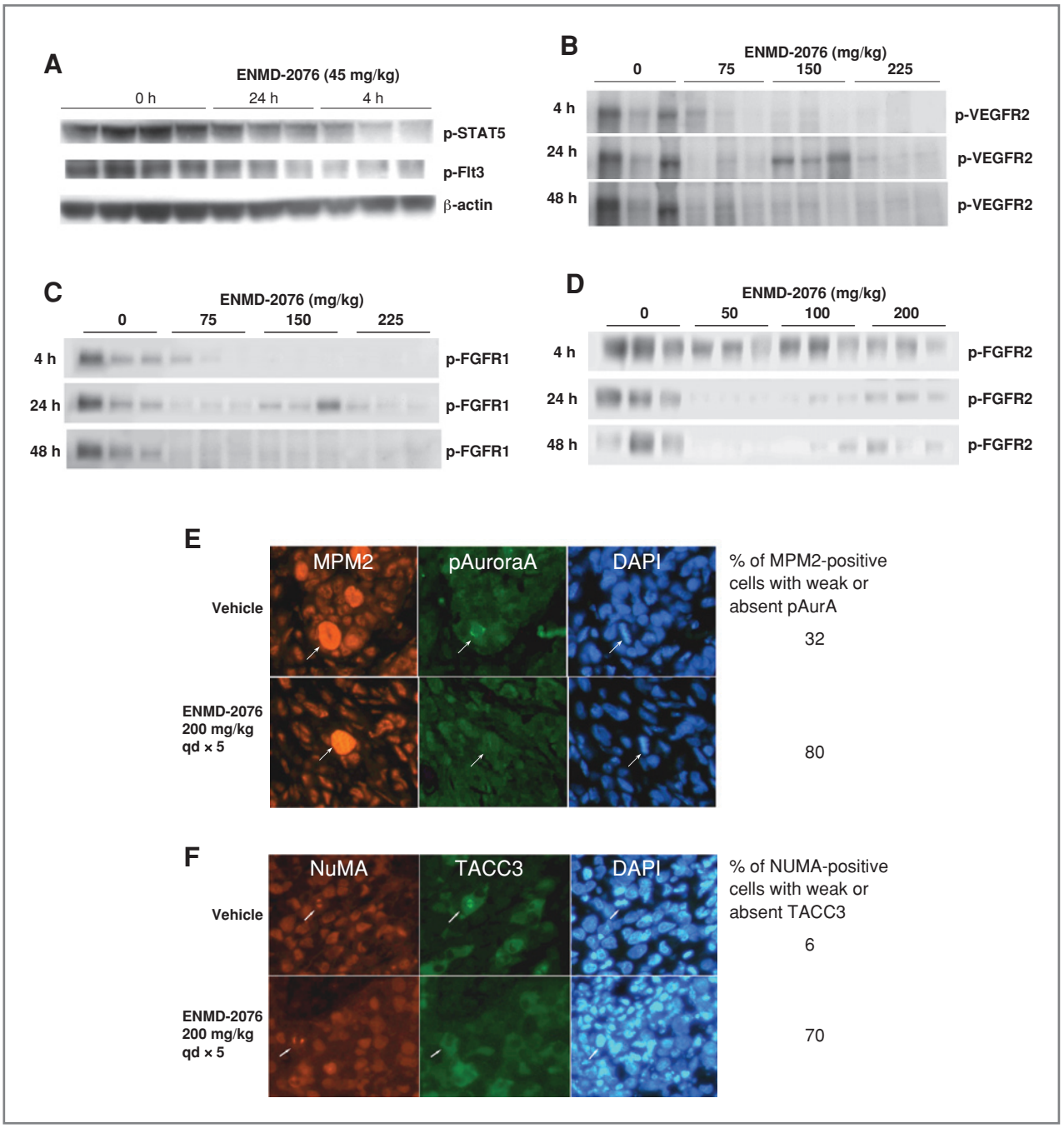


Figure 4. ENMD-2076 inhibits Flt3, VEGFR2/KDR, FGFR-1/2, and Aurora A *in vivo*. A, MV4;11 AML cells ($1 \times 10^7$) suspended in 100μL of Matrigel were injected subcutaneously into female CB.17 SCID mice. Tumor lysates were immunoprecipitated with the 4G10 anti-phosphotyrosine antibody and subjected to Western blotting. Blots were probed with an anti-Flt3 antibody. In addition, whole-tumor lysates were also examined for inhibition of phosphorylated STAT5, a downstream target of Flt3. B and C, MiaPaCa-2 pancreatic carcinoma cells ($5 \times 10^6$) suspended in 100 μL of Matrigel were injected subcutaneously into male NCr nude mice. Tumor lysates were immunoprecipitated with a VEGFR2/KDR antibody (B) or an FGFR1 antibody (C) and then probed with the 4G10 anti-phosphotyrosine antibody. D, KATOIII gastric carcinoma cells ($5 \times 10^6$) in 100 μL of Matrigel were implanted subcutaneously into male NCr nude mice. Tumor lysates were immunoprecipitated with the 4G10 anti-phosphotyrosine antibody and probed with an anti-phosphorylated FGFR2 antibody. A–D, each lane represents material from an individual animal. E and F, ENMD-2076 inhibits Aurora A in an HT29 tumor xenograft model. Animals were treated with 200 mg/kg of ENMD-2076 once a day for 5 days and then 8 hours after the final dose tumors were processed and stained. E, cells stained with MPM2 and DAPI to identify mitotic cells (arrows) in which the level of autoactivated phosphorylated Aurora A was examined. F, cells stained with NuMA and DAPI to identify mitotic cells (arrows) and the Aurora A mediated localization of TACC3 to the centrosomes used to assess Aurora A activity.

Published OnlineFirst December 21, 2010; DOI: 10.1158/1535-7163.MCT-10-0574



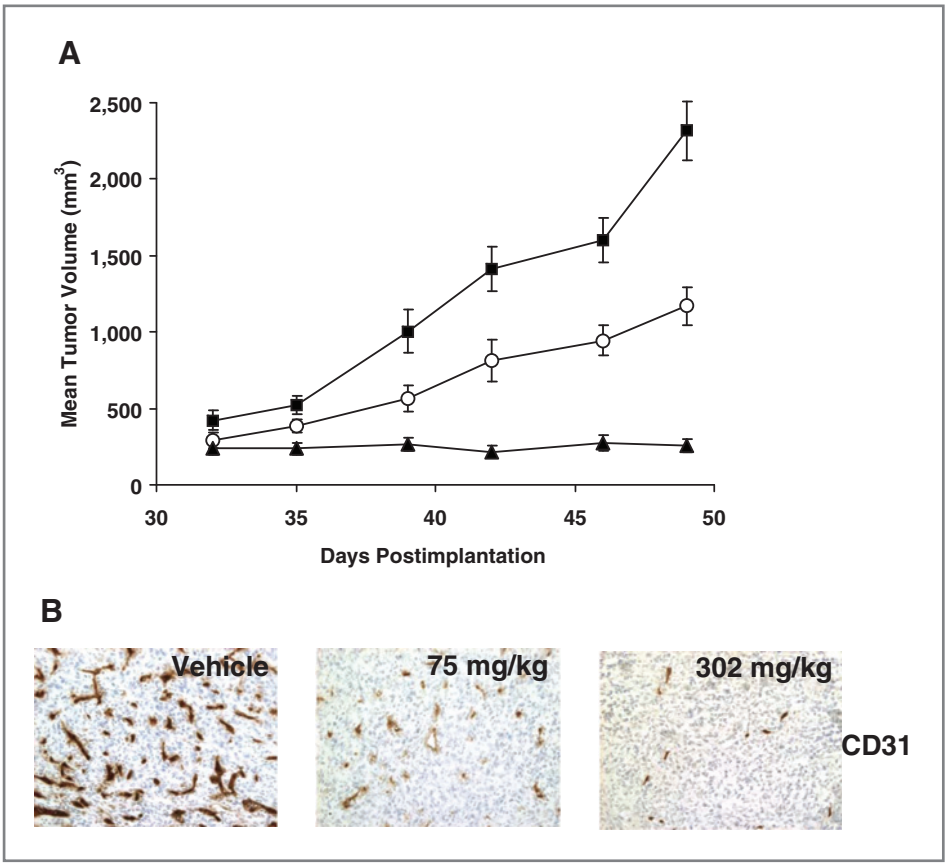


Figure 5. ENMD-2076 inhibits blood vessel formation and impacts the growth of established MDA-MB-231 tumors. A, MDA-MB-231 tumors were implanted in CB.17 SCID mice. Daily oral administration of vehicle (water) or ENMD-2076 at 75 or 302 mg/kg was initiated when tumor volumes reached approximately 300 $mm^3$ and continued to the end of the experiment. (■) vehicle, (○) 75 mg/kg of ENMD-2076, (▲) 302 mg/kg of ENMD-2076. Ten animals were treated per group; bars ± SE. B, CD31 staining in treated tumors harvested 4.5 hours after the final dose.

active cells (29). Five daily doses of ENMD-2076 inhibited TACC3 localization in cells that stained positive for the mitotic marker nuclear mitotic apparatus protein (NuMA; Fig. 4F). Again, 30 mitotic nuclei per condition were counted, and ENMD-2076 treatment increased the percent of NuMA positive cells with low levels of spindle-associated TACC3 from 6% to 70%.

Substantial reduction of tumor growth by ENMD-2076 and the effect of ENMD-2076 on angiogenesis was demonstrated in a xenograft model of the human breast adenocarcinoma MDA-MB-231 (Fig. 5A). Daily oral treatment was initiated 32 days posttumor cell inoculation, when tumors reached an average of 300 $mm^3$. Treatment with 75 mg/kg of ENMD-2076 inhibited tumor growth in this experiment by 54% after 18 days, and treatment with 302 mg/kg almost completely (99%) inhibited tumor growth, with 4 of 10 animals displaying tumors that had regressed to sizes smaller than starting volume (Table 1). At the end of the experiment (18 days of treatment), sections were stained with CD31 to examine the extent of tumor vascularization. A substantial decrease in vessel density was observed at both doses, with a maximal decrease in staining at the 302 mg/kg of dose (Fig. 5B).

## Discussion

ENMD-2076 is the tartrate salt of a novel vinyl pyrimidine chemical entity that originated from an effort to develop inhibitors of the Aurora kinases, which have received considerable attention as potential oncology drug targets in recent years (7, 8, 30). The vinyl pyrimidine core of ENMD-2076 is unique amongst Aurora kinase inhibitors; although, it is a property of the structures of other compounds inhibiting targets such as Tie-2 (31), Src and Abl (32), phosphatidylinositol 3-kinase and mTOR (33). Relative to other clinical stage Aurora kinase inhibitors, ENMD-2076 is most similar structurally to tozasertib (VX-680/MK0457; ref. 24). The differences are in the portion of the molecule, which confers selectivity in inhibitor/target interactions, based on modeling studies (34, 35). The structural changes of ENMD-2076 incorporate a less-derivatized aromatic ring compared with tozasertib (phenyl in ENMD-2076 vs. phenyl-cyclopropanecarboxamide). ENMD-2076 also has a different spacing and angle induced by the linker between the aromatic ring and the pyrimidine core compared with tozasertib (olefin in ENMD-2076 vs. sulfanyl). These changes dramatically differentiate the target profile of the 2 molecules. Unlike tozasertib, which is a pan-Aurora inhibitor (8), ENMD-2076 has greater than 20× selectivity for Aurora A over Aurora B *in vitro* (Table 2) and greater than 3× selectivity in HCT-116 cells (Fig. 2A). Moreover, ENMD-2076 exhibited surprisingly good activity as an orally administered single agent in preliminary xenograft studies in mice,

Published OnlineFirst December 21, 2010; DOI: 10.1158/1535-7163.MCT-10-0574



given its relatively modest growth-inhibitory potency in *in vitro* assays. On this basis, it was hypothesized that ENMD-2076, unlike tozasertib, may also be inhibiting kinases that play significant roles in the growth and support of tumors *in vivo*, such as the angiogenic kinases. This was shown to be the case, as *in vitro* screening showed significant activity toward tyrosine kinases such as Flt3, CSF1R, VEGFR2/KDR, and FGFR2 (Table 3). ENMD-2076 maintained potent inhibitory effects in cellular contexts toward many of the kinases identified as targets through the recombinant panel. Not all of these kinases, however, have the widespread expression across multiple cell types that would account for the broad antitumor efficacy exhibited by ENMD-2076 as a single agent in different preclinical xenograft models. The requirement for the formation and maintenance of a blood supply feeding the tumor is a ubiquitous process in tumorigenesis. The dependence of subcutaneous xenografts on angiogenesis and the ease with which vessels can be quantified in model systems such as the Matrigel plug assay (Fig. 3C and D) have made it relatively more straightforward to assess the contribution of angiogenic kinase inhibition to the overall mechanism of action of ENMD-2076. Robust, potent inhibition of the process of angiogenesis as well as the regression of nascent vessels by ENMD-2076 was shown through a variety of *in vitro* and *in vivo* systems. Pharmacodynamic experiments revealed that the inhibition of receptor tyrosine kinases was dose dependent and of long duration, even after a single oral dose. The importance of the antiangiogenic action to the antitumor effects of ENMD-2076 was also recently shown by Tentler et al. (36), who used DCE-MRI to conclude that the compound induced drastic reductions in vascular perfusion and permeability in the xenografted tumors of treated animals compared with controls, consistent with an antiangiogenic mechanism. It has become increasingly evident that many different kinases are involved in the growth and maintenance of blood vessels, and that specific inhibition of a given kinase, such as VEGFR2/KDR, results in compensatory overexpression of kinases such as the FGFRs (37). This may provide a distinct advantage to agents such as ENMD-2076 that inhibit multiple angiogenic pathways simultaneously.

An important question to address is to what extent the inhibition of kinases within the tumor compartment itself contributes to the mechanism of action of ENMD-2076. The Aurora kinases are ubiquitous in all dividing cells, and their inhibition is likely to explain some of the observed effects of ENMD-2076. ENMD-2076 inhibits Aurora A more potently than Aurora B in *in vitro* kinase assays, and this selectivity is maintained in cell-based kinase assays. In cellular assays, ENMD-2076 produces results characteristic of an Aurora A selective inhibitor, including $G_2$-M arrest, a decrease in the intercentrosomal distance, an increase in the number of monopolar spindles (15) and the induction of apoptosis (Supplementary Figs. S1 and S2). To our knowledge, with the exception of compounds MLN8054 and MLN8237, all of the Aurora inhibitors that have entered clinical studies have been either pan inhibitors of Aurora A and B, or specific Aurora B inhibitors. The significance of this is that the biological outcome of Aurora A and B inhibition is very different (7). It has been postulated that Aurora A may be the preferred target (38), due to the $G_2$-M mitotic arrest and rapid apoptosis that follows its inhibition, relative to the endoreduplication/polyploidy that is a characteristic of Aurora B inhibition or inhibition of both Aurora and Aurora B (12). Indeed, Aurora A is known to be amplified or overexpressed in a number of human cancers (39). There may however be cellular contexts where the cytotoxic effects of Aurora B inhibition may be amplified and therefore desirable such as in cancer cells that are p53 null or mutant (40, 41). In either case, as tolerable serum concentrations of ENMD-2076 are readily achieved in the micromolar range, it is possible that inhibition of Aurora B may occur in the course of treatment. What is not clear at present is how Aurora inhibition may contribute to the overall mechanism of ENMD-2076 *in vivo*, and this is the subject of future experimental effort in both clinical and nonclinical settings.

In summary, ENMD-2076 is a novel, orally active multikinase inhibitor with a mechanism of action that includes inhibition of kinases involved in both angiogenesis and tumor cell proliferation. We have shown that ENMD-2076 exhibits antitumor activity *in vivo* toward a broad range of tumor types as a single agent at well-tolerated doses. Results from a phase 1 study using ENMD-2076 in patients with solid tumors indicate the compound has an acceptable safety profile in humans and clinical benefit is manifested by decreases in tumor volume, reductions in tumor markers, and improvement in cancer-related symptoms in ovarian, colorectal, melanoma, renal cell, neuroendocrine, and hepatocellular cancer patients, even in patients who have received other antiangiogenic treatments (42). A phase 2 trial is currently underway to evaluate the activity of ENMD-2076 in patients with platinum-resistant ovarian cancer.

## Disclosure of Potential Conflicts of Interest

All authors are present or former employees of Entremed Inc. There are no other potential conflicts of interest to disclose.

## Acknowledgments

We extend our thanks to Entremed staff, including Patricia Burke and Kathleen Bengali for doing Western blotting and immunohistochemistry experiments; Steve Strawn for work on xenograft models; and Subodini Perampalam for cellular phosphorylation assays.

The costs of publication of this article were defrayed in part by the payment of page charges. This article must therefore be hereby marked *advertisement* in accordance with 18 U.S.C. Section 1734 solely to indicate this fact.

Received June 24, 2010; revised September 22, 2010; accepted October 31, 2010; published OnlineFirst December 21, 2010.

Published OnlineFirst December 21, 2010; DOI: 10.1158/1535-7163.MCT-10-0574



## References


1. Ma WW, Adjei AA. Novel agents on the horizon for cancer therapy. CA Cancer J Clin 2009;59:111–37.
2. Pytel D, Sliwinski T, Poplawski T, Ferriola D, Majsterek I. Tyrosine kinase blockers: new hope for successful cancer therapy. Anticancer Agents Med Chem 2009;9:66–76.
3. van Erp NP, Gelderblom H, Guchelaar HJ. Clinical pharmacokinetics of tyrosine kinase inhibitors. Cancer Treat Rev 2009;35:692–706.
4. Engelman JA, Settleman J. Acquired resistance to tyrosine kinase inhibitors during cancer therapy. Curr Opin Genet Dev 2008;18:73–9.
5. Pierotti MA, Negri T, Tamborini E, Perrone F, Pricl S, Pilotti S. Targeted therapies: the rare cancer paradigm. Mol Oncol 2010;4:19–37.
6. Nahta R, Esteva FJ. Trastuzumab: triumphs and tribulations. Oncogene 2007;26:3637–43.
7. Carpinelli P, Moll J. Aurora kinases and their inhibitors: more than one target and one drug. Adv Exp Med Biol 2008;610:54–73.
8. Dar AA, Goff LW, Majid S, Berlin J, El-Rifai W. Aurora kinase inhibitors–rising stars in cancer therapeutics?Mol Cancer Ther 2010;9:268–78.
9. Xiao X-Y, Patel DV, Ward JS, Bray MR, Agoston GE, Treston AM, inventors; Miikana Therapeutics Inc. (Rockville, MD), assignee. Substituted pyrazole compounds. United States patent US 7,563,787 . 2006 September 29.
10. Skehan P, Storeng R, Scudiero D, Monks A, McMahon J, Vistica D, et al. New colorimetric cytotoxicity assay for anticancer-drug screening. J Natl Cancer Inst 1990;82: 1107–12.
11. Du J, Hannon GJ. Suppression of p160ROCK bypasses cell cycle arrest after Aurora-A/STK15 depletion. Proc Natl Acad Sci USA 2004;101:8975–80.
12. Yang H, Burke T, Dempsey J, Diaz B, Collins E, Toth J, et al. Mitotic requirement for aurora A kinase is bypassed in the absence of aurora B kinase. FEBS Lett 2005; 579:3385–91.
13. Carmena M, Earnshaw WC. The cellular geography of aurora kinases. Nat Rev Mol Cell Biol 2003;4:842–54.
14. Crosio C, Fimia GM, Loury R, Kimura M, Okano Y, Zhou H, et al. Mitotic phosphorylation of histone H3: spatio-temporal regulation by mammalian Aurora kinases. Mol Cell Biol 2002;22:874–85.
15. Girdler F, Gascoigne KE, Eyers PA, Hartmuth S, Crafter C, Foote KM, et al. Validating aurora B as an anti-cancer drug target. J Cell Sci 2006;119:3664–75.
16. Hoar K, Chakravarty A, Rabino C, Wysong D, Bowman D, Roy N, et al. MLN8054, a small-molecule inhibitor of aurora A, causes spindle pole and chromosome congression defects leading to aneuploidy. Mol Cell Biol 2007;27:4513–25.
17. Levis M, Small D. FLT3: ITDoes matter in leukemia. Leukemia 2003; 17:1738–52.
18. Zhang S, Broxmeyer HE. p85 subunit of PI3 kinase does not bind to human Flt3 receptor, but associates with SHP2, SHIP, and a tyrosine-phosphorylated 100-kDa protein in Flt3 ligand-stimulated hematopoietic cells. Biochem Biophys Res Commun 1999;254:440–5.
19. Lennartsson J, Ronnstrand L. The stem cell factor receptor/c-Kit as a drug target in cancer. Curr Cancer Drug Targets 2006;6:65–75.
20. Smolich BD, Yuen HA, West KA, Giles FJ, Albitar M, Cherrington JM. The antiangiogenic protein kinase inhibitors SU5416 and SU6668 inhibit the SCF receptor (c-kit) in a human myeloid leukemia cell line and in acute myeloid leukemia blasts. Blood 2001;97:1413–21.
21. Guo J, Marcotte PA, McCall JO, Dai Y, Pease LJ, Michaelides MR, et al. Inhibition of phosphorylation of the colony-stimulating factor-1 receptor (c-Fms) tyrosine kinase in transfected cells by ABT-869 and other tyrosine kinase inhibitors. Mol Cancer Ther 2006;5:1007–13.
22. Aharinejad S, Paulus P, Sioud M, Hofmann M, Zins K, Schafer R, et al. Colony-stimulating factor-1 blockade by antisense oligonucleotides and small interfering RNAs suppresses growth of human mammary tumor xenografts in mice. Cancer Res 2004;64:5378–84.
23. Zheng R, Klang K, Gorin NC, Small D. Lack of KIT or FMS internal tandem duplications but co-expression with ligands in AML. Leuk Res 2004;28:121–6.
24. Harrington EA, Bebbington D, Moore J, Rasmussen RK, Ajose-Adeogun AO, Nakayama T, et al. VX-680, a potent and selective small-molecule inhibitor of the Aurora kinases, suppresses tumor growth *in vivo*. Nat Med 2004;10:262–7.
25. Manfredi MG, Ecsedy JA, Meetze KA, Balani SK, Burenkova O, Chen W, et al. Antitumor activity of MLN8054, an orally active small-molecule inhibitor of Aurora A kinase. Proc Natl Acad Sci U S A 2007;104:4106–11.
26. O'Farrell AM, Abrams TJ, Yuen HA, et al. SU11248 is a novel FLT3 tyrosine kinase inhibitor with potent activity *in vitro* and *in vivo*. Blood 2003;101:3597–605.
27. Spiekermann K, Bagrintseva K, Schwab R, Schmieja K, Hiddemann W. Overexpression and constitutive activation of FLT3 induces STAT5 activation in primary acute myeloid leukemia blast cells. Clin Cancer Res 2003;9:2140–50.
28. Kunii K, Davis L, Gorenstein J, Hatch H, Yashiro M, Di Bacco A, et al. FGFR2-amplified gastric cancer cell lines require FGFR2 and Erbb3 signaling for growth and survival. Cancer Res 2008; 68:2340–8.
29. LeRoy PJ, Hunter JJ, Hoar KM, Burke KE, Shinde V, Ruan J, et al. Localization of human TACC3 to mitotic spindles is mediated by phosphorylation on Ser558 by Aurora A: a novel pharmacodynamic method for measuring aurora A activity. Cancer Res 2007;67:5362–70.
30. Kitzen JJ, de Jonge MJ, Verweij J. Aurora kinase inhibitors. Crit Rev Oncol Hematol 2010;73:99–110.
31. Buttar D, Edge M, Emery SC, Fitzek M, Forder C, Griffen A, et al. Discovery of imidazole vinyl pyrimidines as a novel class of kinase inhibitors which inhibit Tie-2 and are orally bioavailable. Bioorg Med Chem Lett 2008;18:4723–6.
32. Zhou T, Commodore L, Huang WS,Wang Y, Sawyer TK, Shakespeare WC, et al. Structural analysis of DFG-in and DFG-out dual Src-Abl inhibitors sharing a common vinyl purine template. Chem Biol Drug Des 2010;75:18–28.
33. Li T, Wang J, Wang X, Yang N, Chen SM, Tong LJ, et al. WJD008, a dual phosphatidylinositol 3-kinase (PI3K)/mammalian target of rapamycin inhibitor, prevents PI3K signaling and inhibits the proliferation of transformed cells with oncogenic PI3K mutant. J Pharmacol Exp Ther 2010;334:830–8.
34. Young MA, Shah NP, Chao LH, Seeliger M, Milanov ZV, Biggs WH, 3rd, et al. Structure of the kinase domain of an imatinib-resistant Abl mutant in complex with the Aurora kinase inhibitor VX-680. Cancer Res 2006;66:1007–14.
35. Zhao B, Smallwood A, Yang J, Koretke K, Nurse K, Calamari A, et al. Modulation of kinase-inhibitor interactions by auxiliary protein binding: crystallography studies on aurora A interactions with VX-680 and with TPX2. Protein Sci 2008;17:1791–7.
36. Tentler JJ, Bradshaw-Pierce EL, Serkova NJ, Hasebroock KM, Pitts TM, Diamond JR, et al. Assessment of the *in vivo* antitumor effects of ENMD-2076, a novel multitargeted kinase inhibitor, against primary and cell line-derived human colorectal cancer xenograft models. Clin Cancer Res 2010;16:2989–98.
37. Casanovas O, Hicklin DJ, Bergers G, Hanahan D. Drug resistance by evasion of antiangiogenic targeting of VEGF signaling in late-stage pancreatic islet tumors. Cancer Cell 2005;8:299–309.
38. Warner SL, Munoz RM, Stafford P, Koller E, Hurley LH, Von Hoff DD, et al. Comparing aurora A and Aurora B as molecular targets for growth inhibition of pancreatic cancer cells. Mol Cancer Ther 2006;5:2450–8.
39. Warner SL, Bearss DJ, Han H, Von Hoff DD. Targeting aurora-2 kinase in cancer. Mol Cancer Ther 2003;2:589–95.
40. Curry J, Angove H, Fazal L, Lyons J, Reule M, Thompson N, et al. Aurora B kinase inhibition in mitosis: strategies for optimising the use of aurora kinase inhibitors such as AT9283. Cell Cycle 2009;8:1921–9.
41. Okada H, Bakal C, Shahinian A, Elia A, Wakeham A, Suh WK, et al. Survivin loss in thymocytes triggers p53-mediated growth arrest and p53-independent cell death. J Exp Med 2004;199:399–410.
42. Bastos BR, Diamond JR, Hansen D, Gustafson J, Arnott J, Bray MR, et al. An open-label, dose escalation, safety, and pharmacokinetic study of ENMD-2076 administered orally to patients with advanced cancer.J Clin Oncol ASCO Annu Meeting Proc (Post-Meeting Ed) 2009;27:3520.

AACR American Association for Cancer Research

Molecular Cancer Therapeutics

# ENMD-2076 Is an Orally Active Kinase Inhibitor with Antiangiogenic and Antiproliferative Mechanisms of Action

Graham C. Fletcher, Richard D. Brokx, Trisha A. Denny, et al.

*Mol Cancer Ther* 2011;10:126-137. Published OnlineFirst December 21, 2010.